

CENTERIS - International Conference on ENTERprise Information Systems /
ProjMAN - International Conference on Project MANagement / HCist - International
Conference on Health and Social Care Information Systems and Technologies,
CENTERIS/ProjMAN/HCist 2018

Monitoring continuous subsidence in the Costa del Sol (Málaga province, southern Spanish coast) using ERS-1/2, Envisat, and Sentinel-1A/B SAR interferometry

Antonio M. Ruiz-Armenteros^{a,b,c,*}, Milan Lazecky^d, Ana Ruiz-Constán^e, Matúš Bakoň^{f,g},
J. Manuel Delgado^c, Joaquim J. Sousa^h, Jesús Galindo-Zaldívarⁱ,
Carlos Sanz de Galdeano^j, Miguel Caro-Cuenca^k, Sergio Martos-Rosillo^e,
Pablo Jiménez-Gavilán^l, and Daniele Perissin^m

^aDpto. Ingeniería Cartográfica, Geodésica y Fotogrametría, Univ. Jaén, EPSJ, Campus Las Lagunillas s/n, Edif. A3, 23071 Jaén, Spain

^bCentro de Estudios Avanzados en Ciencias de la Tierra CEA-Tierra, Universidad de Jaén, Spain

^cGrupo de investigación Microgeodesia Jaén, Universidad de Jaén, Spain

^dIT4Innovations, VSB-TU Ostrava, Czech Republic

^eInstituto Geológico y Minero de España, Urb. Alcázar del Genil 4, Edif. Zulema, 18006 Granada, Spain

^fUniversity of Presov in Presov, Fac. of Management, Dept. of Environmental Management, Konstantinova 16, 080 01 Presov, Slovak Republic

^ginsar.sk s.r.o., Lesna 35, 080 01 Presov, Slovak Republic

^hUTAD, Vila Real and INESC-TEC (formerly INESC Porto), Portugal

ⁱDepartamento de Geodinámica, Universidad de Granada, 18071 Granada, Spain

^jInstituto Andaluz de Ciencias de la Tierra, CSIC-Universidad de Granada, 18071 Granada, Spain

^kDepartment of Radar Technology, TNO, The Netherlands

^lDepartamento de Ecología y Geología, Facultad de Ciencias, Universidad de Málaga, Málaga, Spain

^mLyles School of Civil Engineering, Purdue University, West Lafayette, IN47907, USA

Abstract

In this paper we analyze the subsidence behavior of a coastal area in the province of Málaga (Costa del Sol), southern Spain, in the period 1992–2018 using C-band SAR interferometry. The area comprises several zones of interest where continuous deformation has happened during the analyzed period. Using SAR data from ESA's ERS-1/2, Envisat, and Sentinel-1A/B satellites, and Multi-Temporal InSAR methods we detect and monitor subsidence in highly populated and industrial areas,

* Corresponding author. Tel.: +34 953 218 851; fax: +34 953 212 854

E-mail address: amruiz@ujaen.es

airport, harbor, as well as local instabilities over a railway line and a highway. In a previous work, we reported a subsidence due to intensive use of groundwater in some populated towns in the period 1992–2009 with maximum line-of-sight (LOS) rates of the order of -11 mm/yr. In this contribution, we confirm the subsidence trend. Furthermore, we detect an increase in the deformation rates for the most recent period (2014–2018), suggesting that the overexploitation of the aquifers has not ceased.

© 2018 The Authors. Published by Elsevier Ltd.

This is an open access article under the CC BY-NC-ND license (<https://creativecommons.org/licenses/by-nc-nd/4.0/>)

Selection and peer-review under responsibility of the scientific committee of the CENTERIS - International Conference on ENTERprise Information Systems / ProjMAN - International Conference on Project MANagement / HCist - International Conference on Health and Social Care Information Systems and Technologies.

Keywords: Málaga; Torremolinos; InSAR; Deformation; Sentinel-1; ERS-1/2; Envisat; SAR.

1. Introduction

Increase in population and water use in several cities worldwide causes overexploitation of aquifers as groundwater extraction provides an alternative solution for accessing a fresh water supply. Land subsidence induced by overexploitation of groundwater resources can lead to harmful effects like damage to infrastructure and buildings, changes in elevation of water streams, and other failures in aquifer system. In coastal areas, long-term excessive extraction of groundwater and resulting subsidence might cause tides moving into lower altitude areas that were previously above higher tide levels. In this work, we focus on the coastal area of southern Spain, more precisely on the Costa del Sol, in the province of Málaga. We apply spaceborne Synthetic Aperture Radar (SAR) instruments to identify and measure land subsidence.

Spaceborne SAR has proven to be an excellent technique for studying ground motion caused by underground water flow of large areas^{1,2,3,4}. In a previous work, we had already identified subsidence in several areas of the Costa del Sol⁵ applying Multi-Temporal InSAR techniques (MT-InSAR) to an ERS-1/2 SAR dataset (1992–2000) through the Stanford Method for Persistent Scatterers Multi-Temporal Interferometry (StaMPS MT-InSAR). The subsidence was mainly located in the towns of Benalmádena, Torremolinos, and in the SW of Málaga (study area represented in Fig. 1). These subsidence patterns were afterwards confirmed for the 2003–2008 period, through the processing of an Envisat ASAR dataset with the SBAS InSAR Service of European Space Agency's Geohazard Exploitation Platform (GEP), an unsupervised MT-InSAR analysis⁶. We then analyzed⁷ the water level evolution of the aquifers supplying freshwater to the towns of Torremolinos and Benalmádena, the so-called Sierra de Mijas and Bajo Guadalhorce aquifers (carbonate and detritic aquifers, respectively), to determine their degree of overexploitation during the 1992–2009 period, when the major population increase took place. ERS-1/2 and Envisat as well as hydrological data were used in the reported study. We measured an accumulated deformation of -102 mm, with maximum displacement rates of -6 mm/yr (1992–2000) and -11 mm/yr (2003–2009). We found a good temporal correlation between subsidence and the piezometric level of the carbonate confined aquifer, suggesting that deformation was due to the decrease in interstitial pressure caused by overexploitation.

In this paper, we expand our previous work. We apply spaceborne SAR interferometry to estimate and analyze ground motion in the Benalmádena-Torremolinos area using C-band SAR images from the European ERS-1/2 (1992–2000), Envisat (2003–2009), and Sentinel-1A/B (2014–2018) satellites to monitor the subsidence in a time span of almost 30 years.

2. Geological settings

The study area, located in southern Spain, comprises the Málaga Basin (Fig. 1) and the reliefs surrounding it (Sierra de Mijas, Sierra de Cártama, and Montes de Málaga). The sedimentary sequence of the basin is constituted by Miocene to Quaternary sediments⁸ cropping out at the depression where the Guadalhorce River flows and continuing offshore. Its basement is formed by the Triassic marbles—and the Paleozoic rocks under them—of Sierra de Mijas and Sierra de Cártama, in the southern and central sectors; northwards, the basement is constituted by Paleozoic slates and greywackes of Montes de Málaga and, tectonically over them, Cretaceous-Tertiary flysch

clays, also including lower Miocene formations (Figs. 1 and 2). From a hydrogeological point of view, the study area comprises part of the aquifers of Sierra de Mijas (carbonate aquifer) and Bajo Guadalhorce (multi-layered detritic aquifer). The permeability of the calcareous massif is mainly related to fractures and karstification processes⁹. The carbonate aquifer recharge stems from rainfall infiltration meanwhile present-day discharge is mainly related to pumping activity¹⁰, but also to lateral flow to the Bajo Guadalhorce detritic aquifer. Recharge of Sierra de Mijas is estimated in $\sim 28 \text{ hm}^3/\text{yr}$, while pumping is around $35 \text{ hm}^3/\text{yr}$ ¹¹, surpassing the resources of the system and causing an accumulated water table decrease of 80-100 m in the period 1997-2003⁹ and the subsequent disappearance of most of the springs. On the other hand, pumping well depths at the detritic aquifer are generally lower than 50 m and water is mainly obtained from the Quaternary alluvial aquifer¹¹ without an accumulated water table decrease. The spatio-temporal analysis of the subsidence evolution (1992 and 2009) in the Torremolinos-Benalmádena sector, probed that its pattern is well correlated with the carbonate water-table evolution, pointing to the interstitial pressure decrease due to water withdrawal as the main subsidence triggering factor⁷.

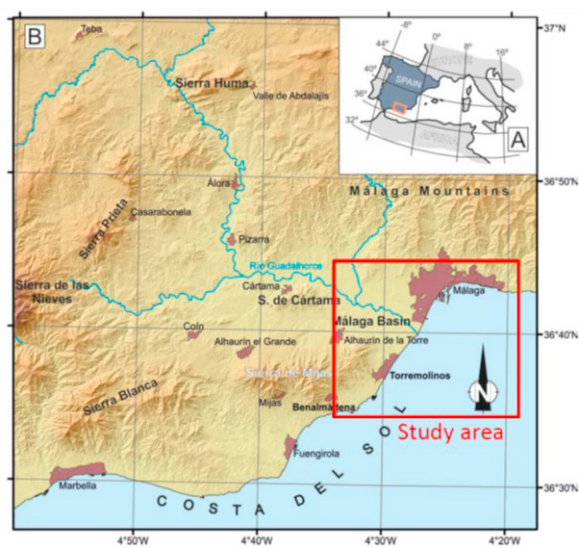


Fig. 1. Location of the study area in the southern Spanish coast.

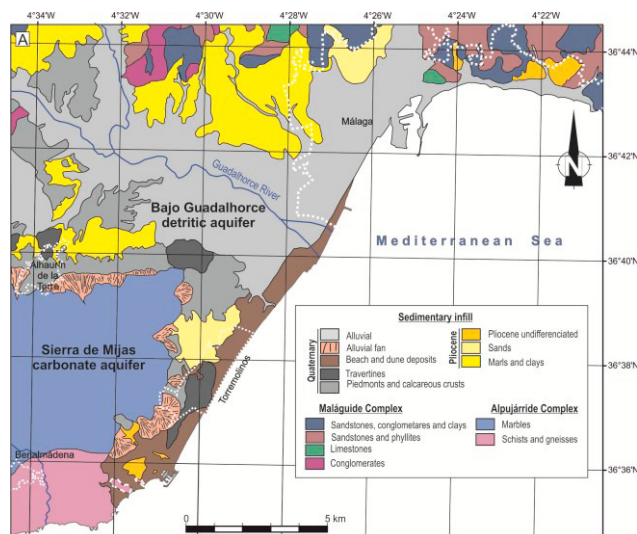


Fig. 2. Geological map of Sierra de Mijas carbonate aquifer and Bajo Guadalhorce detritic aquifer. Modified from 1066 and 1067 MAGNA 50 geological maps^{12,13}. White dotted-lines represent the location of the main towns while white dashed-line indicates the sediment/basement boundary.

3. Data and Method

3.1. Data

The SAR dataset used in this study was composed of 176 images acquired by three C-band ($\sim 5.7 \text{ cm}$ wavelength) satellites sensors, covering the total time period from May 1992 to February 2018. We used 30 ERS-1/2 SLC SAR images (ascending orbits, track 230) with an incident angle of 23° and a $5 \times 25 \text{ m}$ nominal spatial resolution (azimuth x range), 20 Envisat ASAR images (ascending orbits - track 230), acquired with an incidence angle of 23° at the middle swath IS2, and a $5 \times 25 \text{ m}$ nominal pixel dimension (azimuth x range), and 126 Sentinel-1A/B IW SLC SAR images (86 Sentinel-1A and 40 Sentinel-1B, acquired in descending orbits) with an incidence angle of $37\text{--}39^\circ$ in the center of sub-swath 2 and a pixel spacing of $2.3 \times 14.1 \text{ m}$ (range x azimuth).

3.2. Multi-Temporal InSAR

SAR interferometry (InSAR) allows scanning the Earth surface regularly with a given (usually fixed) revisit time. Although InSAR has proven to be a very valuable geodetic tool, the technique has some limitations. InSAR is affected by temporal and geometrical decorrelation. In order to overcome these limitations, several MT-InSAR approaches were developed in the last years. All of these techniques exploit multiple SAR images acquired over the same area and apply appropriate data processing and analysis procedures to separate the contribution of the phase caused by the deformation from the other phase components. The technique focuses on the identification of pixels in the SAR image characterized by small noise, which are typically related to two types of reflectors: those whose radar response is dominated by a strong reflecting object and remains constant over time (Persistent Scatterer, PS) and those whose response is relatively constant over time, but is due to different small scattering objects (Distributed Scatterers, DS) or SDFP (slowly decorrelating filtered phase). The detection and exploitation of these two type of pixels define two broad categories of MT-InSAR techniques, the persistent scatterer (PSI) methods (e.g.^{14,15,16}) and the small baseline (SB) methods (e.g.^{17,18}).

In this study, we use for comparison purposes two software packages in the processing of the SAR datasets, StaMPS and SARPROZ.

We process ERS-1/2, Envisat datasets using StaMPS¹⁵, more specifically its extended version (StaMPS-MTI) that includes a combined MT-InSAR method, allowing the identification of both PS and SDFP pixels. The processing chain uses the typical single master scene approach (August 13, 1997 for the ERS-1/2 dataset and February 2, 2005 in the case of Envisat). In order to compute the PS probability for individual pixels allowing the identification of stable points, StaMPS uses both amplitude and phase analysis. First, an initial selection based only on amplitude analysis is performed, and then the PS probability is refined using phase analysis in an iterative process. Comparing to standard PSI approach^{14,16}, StaMPS does not require any *a priori* assumptions about the temporal nature of the deformation for PS selection, since it uses the spatially correlated nature of deformation rather than requiring a known temporal dependence. StaMPS SB approach uses the amplitude dispersion values and then identifies the SDFP pixels performing the phase analysis in space and time. In this way, both types of selected points (PS + SDFP) are combined and the deformation signal is separated by the application of a 3D phase unwrapping algorithm. In this study, StaMPS – MTI (combined processing) was applied to both ERS-1/2 and Envisat datasets.

In addition, we apply the PSI method implemented in SARPROZ¹⁹ to the set of Sentinel-1A/B radar images with which we estimate the Atmospheric Phase Screen (APS) to improve the quality of the phase signal. PS candidates were chosen by applying threshold on the Amplitude Stability Index, following the standard PSInSAR processing¹⁴. For the selected points, height and displacement were estimated and deformation time series were reconstructed. The image of January 16, 2017 was chosen as the master for the single master processing.

Finally, we process the Sentinel-1A/B dataset with one more approach referred to as IT4S1²⁰. In this case, the Sentinel-1A/B data are specifically preprocessed using the InSAR Scientific Computing Environment (ISCE)²¹. Coregistration process together with the necessary fine corrections and also topography and flat Earth phase removal have been performed directly to the SLC data. Afterwards, interferometric combinations were prepared for PSI processing using StaMPS.

For all datasets above mentioned, we use as the reference area a stable zone in the city of Málaga.

4. Results and conclusions

Fig. 3 shows the mean LOS velocity maps derived from ERS-1/2 (1992-2000), Envisat (2003-2009), Sentinel-1A/B SARPROZ (2014-2018), and Sentinel-1A/B ISCE-StaMPS processing, related to the reference area located in the city of Málaga. The stability of the reference area has been showed in previous tests. The ERS-1/2 and Envisat results correspond to the combined (PSI+SB) processing carried out with StaMPS whereas the Sentinel-1A/B results come from the PSI processing done with SARPROZ and ISCE-StaMPS.

From a general point of view, we observe different subsiding areas but with different deforming rates depending on the analyzed period. The first area corresponds to Torremolinos and Benalmádena towns close to the coast. They are shown in a greater detail in Fig. 4. We presented results of a subsidence bowl in this area for the period 1992-

2009⁷. Using the most recent images, we detected that the subsidence bowl has increased for the period 2014–2018, which denotes that an intensive use of the underground water could be still taking place.

The second area, shown in Fig. 5, reveals the subsidence occurred in the industrial area (Polígono Industrial Guadalhorce) located southwest of Málaga city. This can be clearly seen in the ERS-1/2 and Envisat periods but lately, it seems to be displaced to the south as it is evidenced by the Sentinel-1A/B analysis, affecting even the Málaga international airport (Málaga-Costa del Sol airport), an important airport for Spanish tourism as it is the main airport serving the Costa del Sol. In addition, we detected some subsidence in the harbor during the Envisat period, having been stabilized at a later time as it is evidenced by the Sentinel-1A/B analysis. However, a new small area appears to be prone to subsidence, corresponding to the most recent reclaimed land for expanding port facilities.

Finally, the third crop, shown in Fig. 6, reveals another subsidence bowl located in a residential area located in Alhaurín de la Torre village. As with Torremolinos-Benalmádena area, the deformation in Alhaurín de la Torre appears to be increasing with time as revealed by the evolution of the subsidence pattern during the three analyzed periods. Additionally, we detected a small subsidence, slightly with ERS-1/2 and increased with Envisat, between the north of Castañetas and east of Santa Rosalía, two neighborhoods of Málaga city (20 km from the center) located in the district of Campanillas and very close to the banks of the Guadalhorce River. This subsidence now appears to have been stabilized in the Sentinel-1A/B period (upper part of Fig. 7). Furthermore, during the last analyzed period (2014–2018), there seems to be some deformation of the railway line and in a highway near Málaga in the area of Fig. 7, marked with ellipses. However, this deformation signals need to be further investigated.

The accuracy of PS InSAR results is a function of the number of available images¹⁴. Original works related to PS show a good reliability using ~ 30 images¹⁴ while it is expected to achieve accuracy ~ 0.2 mm/yr in estimation of displacement velocity for PS points having coherence > 0.7 if the number of C-band sensor images is around 100^2 . The performance of MT-InSAR in less urbanized areas is typically lower, however the specific approach¹⁵ we have applied should keep the results reliable also in such areas, though small spatial scale motion may get neglected¹⁷. Future work will complete this research analyzing some other information as rainfall, water tables, and gravity data when they become available. All this analysis will allow a better understanding of the sources of this subsidence.

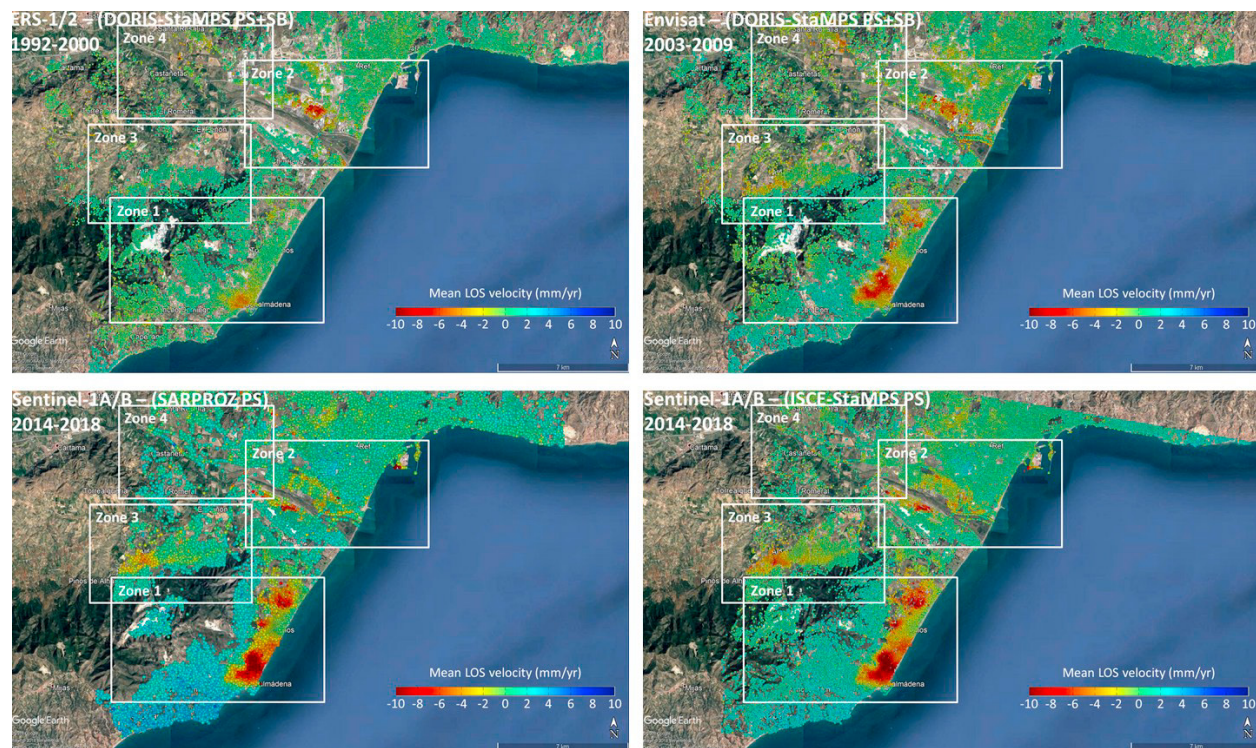


Fig. 3. Mean LOS velocity of the study area.

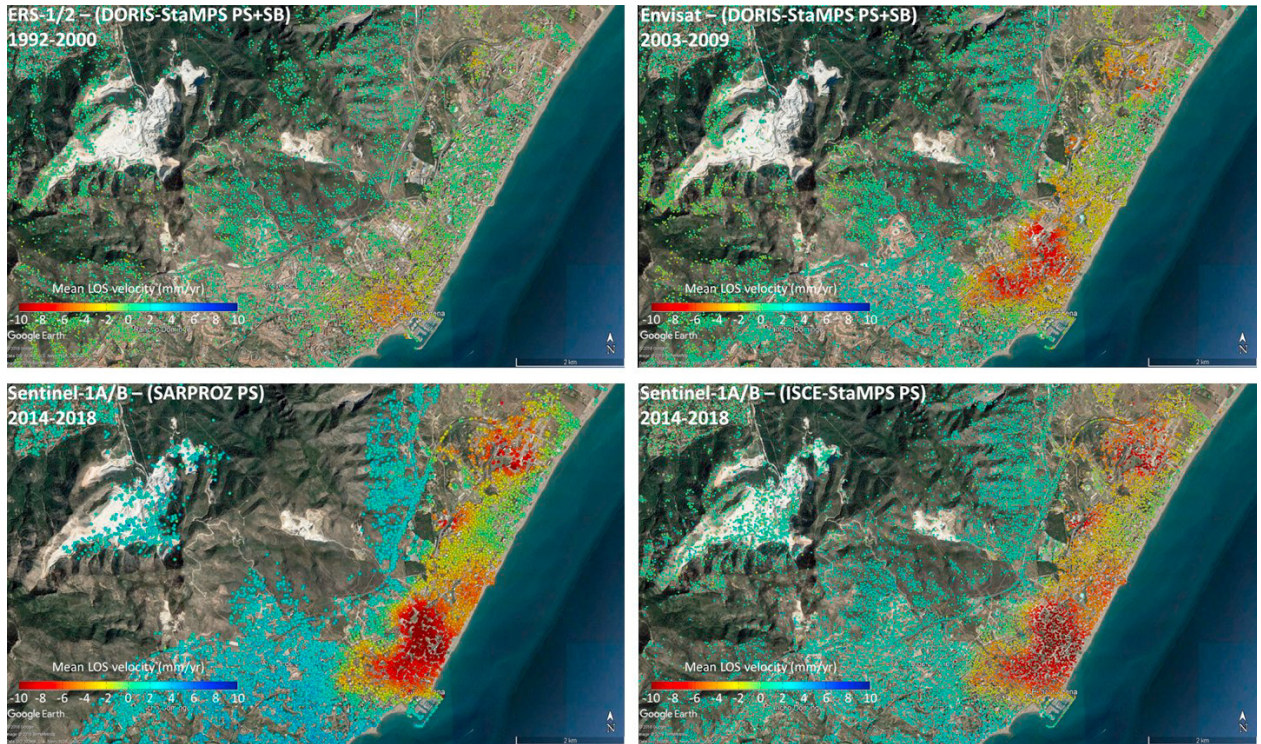


Fig. 4. Mean LOS velocity of the zone 1 (Fig. 3) corresponding to Torremolinos-Benalmádena area.

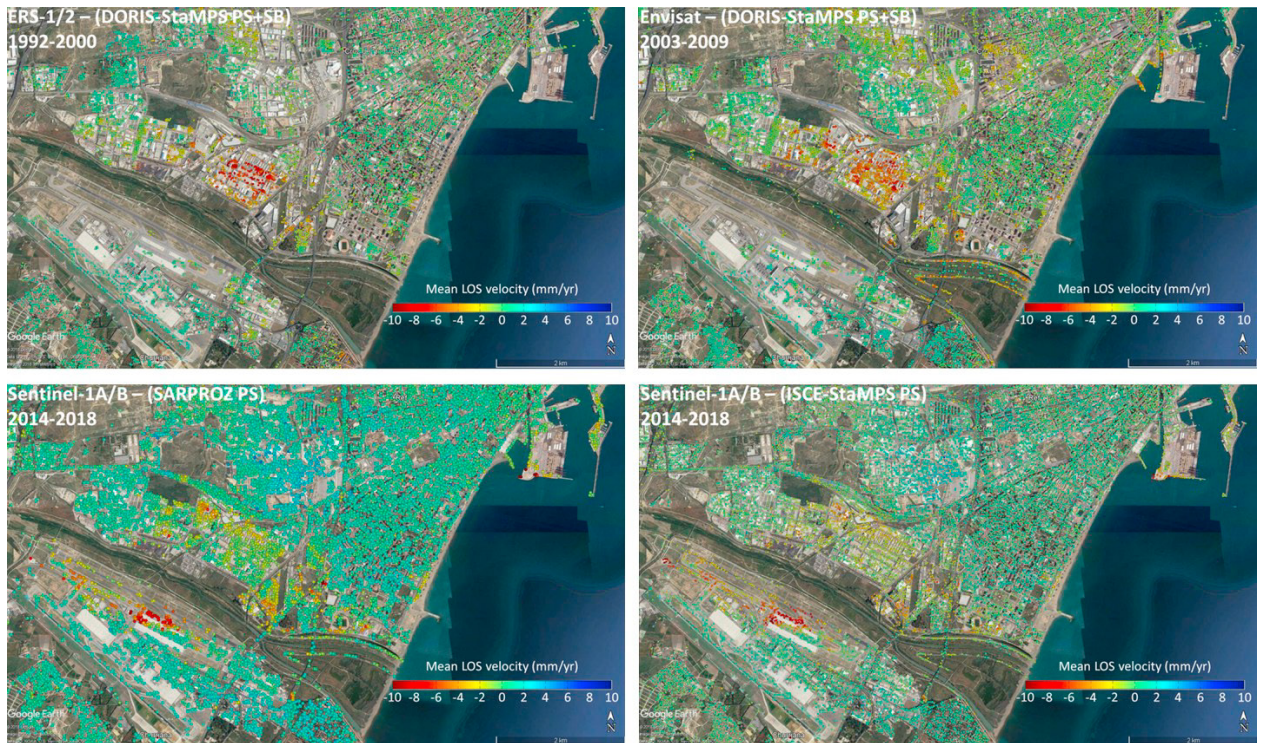


Fig. 5. Mean LOS velocity of the zone 2 (Fig. 3) corresponding to an industrial area (Polígono Industrial Guadalhorce), the Málaga international airport (Málaga-Costa del Sol), and the harbor.

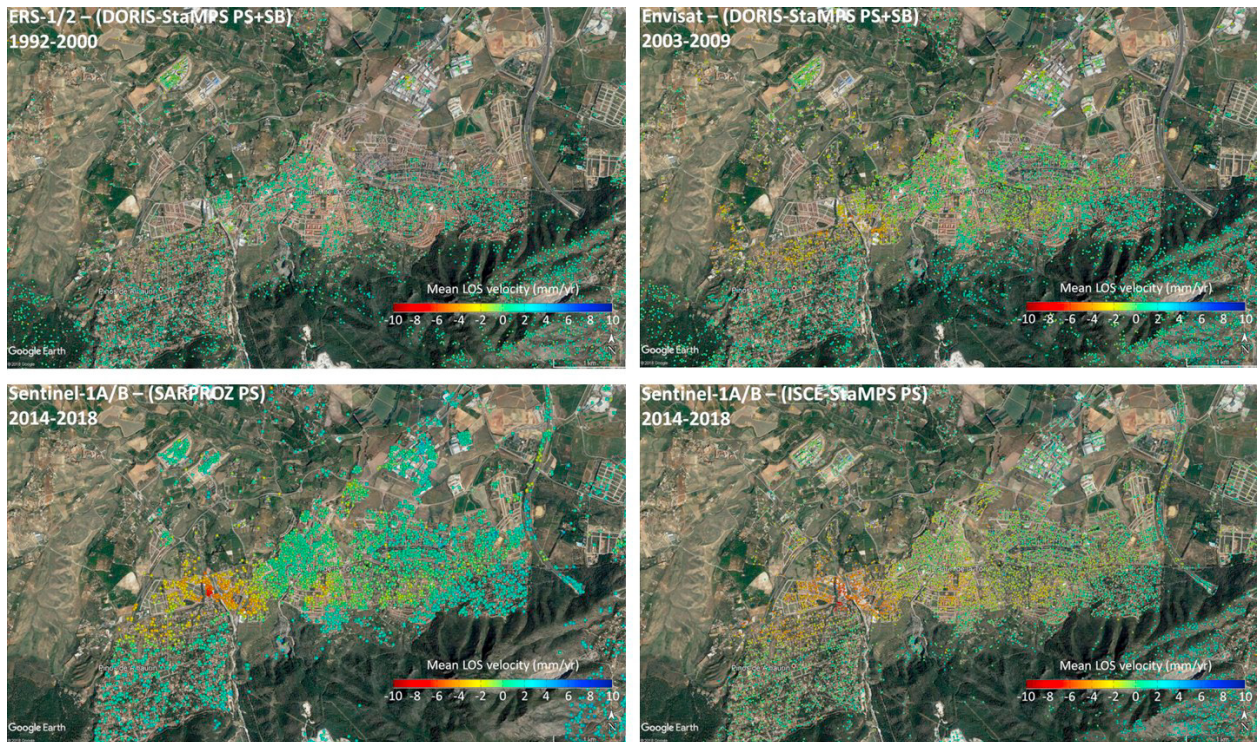


Fig. 6. Mean LOS velocity of the zone 3 (Fig. 3) corresponding to Alhaurín de la Torre village.

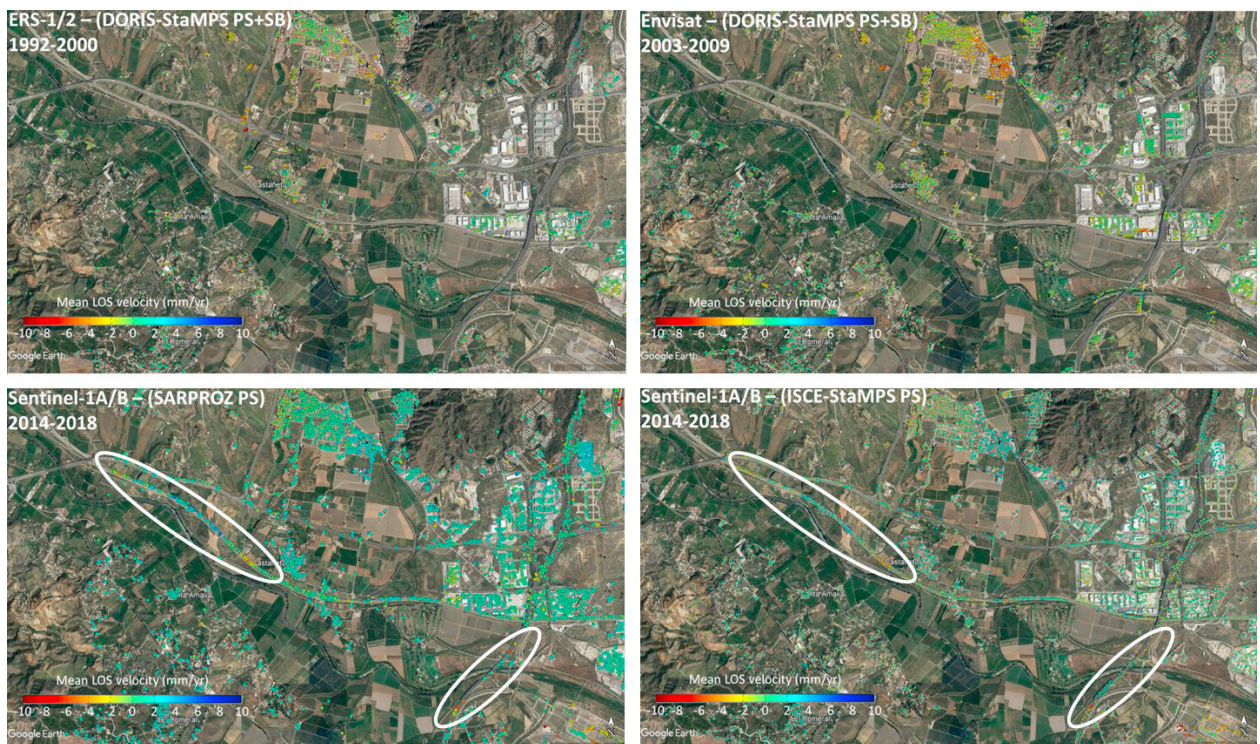


Fig. 7. Mean LOS velocity of the zone 4 (Fig. 3) corresponding to a railway line and a highway.

Acknowledgements

ERS-1/2 and Envisat data were provided by the European Space Agency (ESA) within 28654 G-POD and 7629 CAT-1 projects. Sentinel-1A/B data were freely provided by ESA through Copernicus Programme. Satellite orbits are from TU Delft and ESA. Data processed by DORIS from TU Delft, StaMPS, SARPROZ, ISCE from NASA/JPL and G-POD service of ESA. Research was supported by: (a) ESA Research and Service Support for providing hardware resources employed in this work, (b) PAIUA-2017/2018 and CEACTierra from University of Jaén (Spain), and RNM-282 research group from the Junta de Andalucía (Spain), (c) ERDF through the Operational Programme for Competitiveness and Internationalisation - COMPETE 2020 Programme within project «POCI-01-0145-FEDER-006961», and by National Funds through the FCT – Fundação para a Ciência e a Tecnologia (Portuguese Foundation for Science and Technology) as part of project UID/EEA/50014/2013, (d) The Ministry of Education, Youth and Sports from the National Programme of Sustainability (NPU II) project «IT4Innovations excellence in science - LQ1602» (Czech Republic), and (e) Slovak Grant Agency VEGA under projects No. 1/0714/15 and 1/0462/16.

References

- [1] Hoffmann, J., Zebker, H., Galloway, D., and Amelung, F. (2001) “Seasonal subsidence and rebound in Las Vegas Valley, Nevada, observed by synthetic aperture radar interferometry”. *Water Resources Research* **37**, 1551–1566.
- [2] Colesanti, C., Ferretti, A., Novali, F., Prati, C., Rocca, F. (2003) “SAR monitoring of progressive and seasonal ground deformation using the permanent scatterers technique”. *IEEE Transactions on Geoscience and Remote Sensing* **4**, 1685–1701.
- [3] Schmidt, D.A., and Burgmann, R. (2003) “Time-dependent land uplift and subsidence in the Santa Clara valley, California, from a large interferometric synthetic aperture radar data set”. *Journal of Geophysical Research* **108**, 2416–2428. <https://doi.org/10.1029/2002JB002267>.
- [4] Caro Cuenca, M. (2012) “Improving Radar Interferometry for Monitoring Fault-Related Surface Deformation: Application for the Roer Valley Graben and CoalMine Induced Displacements in the Southern Netherlands”. Ph. D. Thesis. Delft University of Technology.
- [5] Ruiz, A.M., Caro Cuenca, M., Sousa, J.J., Gil, A.J., Hanssen, R.F., Perski, Z., Galindo-Zaldívar, J., and Sanz de Galdeano, C. (2011) “Land subsidence monitoring in the southern Spanish coast using satellite radar interferometry”. *FRINGE 2011*, Frascati, 19–23 Sep 2011, 19–23.
- [6] Galve, J.P., Pérez-Peña, J.V., Azañón, J.M., Closson, D., Caló, F., Reyes-Carmona, C., Jabaloy, A., Ruano, P., Mateos, R.M., et al. (2017). “Evaluation of the SBAS InSAR Service of the European Space Agency's Geohazard Exploitation Platform (GEP)”. *Remote Sensing* **9**, 1291.
- [7] Ruiz-Constán, A., Ruiz-Armenteros, A.M., Martos-Rosillo, S., Galindo-Zaldívar, J., Lazecky, M., García, M., Sousa, J.J., Sanz de Galdeano, C., Delgado-Blasco, J.M., Jiménez-Gavilán, P., Caro-Cuenca, M., Luque-Espinar, J.A. (2018). “SAR interferometry monitoring of subsidence in a detritic basin related to water depletion in the underlying confined carbonate aquifer (Torremolinos, southern Spain)”. *Science of the Total Environment* **636**, 670–687.
- [8] IGME, (1983). “Investigación hidrogeológica de las cuencas del Sur de España. Sistema acuífero nº 37 “Detritico de Málaga”. Technical report nº 5”. http://www.igme.es/sistemas_infor/Sid.htm, Accessed date: 1 May 2018.
- [9] Andreo, B. (2007). “Sierra de Mijas”. In: Durán-Valsero, J.J. (Ed.), (Coord), Atlas hidrogeológico de la provincia de Málaga. Instituto Geológico y Minero de España and Diputación de Málaga, pp. 173–178.
- [10] Andreo, B., Carrasco, F., Vadillo, I., Liñán, C. (1996). “Características hidrogeológicas de las Sierras Blanca y Mijas (Provincia de Málaga, Cordillera Bética)”. *Geogaceta* **20(6)**, 1267–1270.
- [11] BOE (2016). “Real Decreto 11/2016, de 8 de enero, por el que se aprueban los Planes Hidrológicos de las demarcaciones hidrográficas de Galicia-Costa, de las Cuencas Mediterráneas Andaluzas, del Guadalete y Barbate y del Tinto, Odiel y Piedras”. *Boletín Oficial del Estado* 2016 19:6082–6084. <https://www.boe.es/boe/dias/2016/01/22/pdfs/BOE-A-2016-602.pdf>.
- [12] PilesMateo, E., Estévez-González, C., and BarbaMartin, A. (1978). “Mapa Geológico de España 1:50.000 MAGNA. Hoja nº 1066, Coin”. Instituto Geológico y Minero de España, Madrid.
- [13] Estévez-González, C., Chamón Cobos, C. (1978). “Mapa Geológico de España 1:50.000 MAGNA. Hoja nº 1067, Torremolinos”. Instituto Geológico y Minero de España, Madrid.
- [14] Ferretti, A., Prati, C., and Rocca, F. (2001) “Permanent Scatterers in SAR Interferometry”. *IEEE Transactions on Geoscience and Remote Sensing* **39(1)**: 8–20.
- [15] Hooper, A., Zebker, H., Segall, P., and Kampes, B. (2004) “A new method for measuring deformation on volcanoes and other natural terrains using InSAR persistent scatterers”. *Geophysical Research Letters* **31**: L23611. <http://dx.doi.org/10.1029/2004GL021737>.
- [16] Kampes, B.M. (2006) “Radar Interferometry: Persistent Scatterer Technique”, Kluwer Academic Publishers, Dordrecht, The Netherlands.
- [17] Berardino, P., Fornaro, G., Lanari, R., and Sansosti, E. (2002) “A new algorithm for surface deformation monitoring based on small baseline differential SAR interferograms”. *IEEE Transactions on Geoscience and Remote Sensing* **40(11)**, 2375 – 2383.
- [18] Schmidt, D.A., and Burgmann, R. (2003) “Time-dependent land uplift and subsidence in the Santa Clara valley, California, from a large interferometric synthetic aperture radar data set”. *Journal of Geophysical Research* **108**, B9: 2416–2428.
- [19] Perissin, D. (2015) “SARPROZ software”. Official Product Web page: <http://www.sarproz.com>.
- [20] Lazecky, M. (2017) “System for Automatized Sentinel-1 Interferometric Monitoring”, 4 p., Proc. of ESA BIDS, Toulouse, 28-30 Nov 2017
- [21] Rosen, P., Gurrola, E., Agram, P. S., Sacco, G. F. and Lavalle, M. (2015) “InSAR Scientific Computing Environment (ISCE): A Python Framework for Earth Science”, AGU Fall Meeting 2015.